ESANN 2024 proceedings, European Symposium on Artificial Neural Networks, Computational Intelligence and Machine Learning. Bruges (Belgium) and online event, 9-11 October 2024, i6doc.com publ., ISBN 978-2-87587-090-2.
Available from http://www.i6doc.com/en/.

EEG Source Imaging Enhances Motor Imagery Classification

Andres Soler[1], Viktor Naas[1], Amita Giri[2] and Marta Molinas[1]

[1]Department of Engineering Cybernetics,
Norwegian University of Science and Technology, Trondheim, Norway.

[2]Department of Brain and Cognitive Sciences,
Massachusetts Institute of Technology, Boston, USA

Abstract. Brain-computer Interfaces (BCIs) have been developed towards enhancing communication and control in individuals with motor disabilities and assist in motor rehabilitation, where motor imagery (MI), the mental visualization of limb movement, has been broadly explored. Traditionally, MI-based BCIs utilize electroencephalographic (EEG) recordings to discriminate between limbs motor imagination. This involves applying feature extraction and classification, primarily analyzing signals recorded at the scalp. Despite the success of the traditional sensor space analysis, recent studies have demonstrated that incorporating EEG source imaging (ESI) has led to an improvement of the classification performance. This work studies pipelines on both sensor and source space for classifying upper limb MI. Here, we introduce the use of source average power for the integration of ESI into MI-based BCIs. Our results suggest a significant accuracy improvement of 10% when applying source space analysis with average power against traditional sensor space analysis. This demonstrates that a shift from sensor space analysis to source space analysis can be beneficial for MI classification.

Index Terms - EEG, BCI, Motor Imagery, EEG Source Imaging, Source Reconstruction, Average Power.

1 Introduction

A Brain-Computer Interface (BCI) is a computer system which analyzes signals from the brain, such as the electrical fields measured by Electroencephalography (EEG), to use as communication between a human and a computer [1]. The EEG technique has been broadly adopted in BCI systems due to its non-invasive nature, affordability, portability, and high temporal resolution. These qualities position EEG as a promising choice for the sensors required in a BCI system.

In a Motor Imagery (MI) based BCI, users imagine the kinesthetic sensation associated with moving specific limbs. The BCI system then analyzes the recorded EEG signals, using them as the control input for the BCI. MI-based BCI holds promise for various clinical applications, including reducing phantom limb pain [2] and rehabilitating limb movement in ischemic stroke patients [3]. Before reaching classification, the EEG is usually pre-processed, by removing unwanted artifacts, then filtered in frequencies of interest, and the features to discriminate between different types of imagined movements are extracted.

Artifacts are often removed manually or semi-automatically with Independent Component Analysis (ICA) [4]. ICA is considered the safest way to correct

ESANN 2024 proceedings, European Symposium on Artificial Neural Networks, Computational Intelligence and Machine Learning. Bruges (Belgium) and online event, 9-11 October 2024, i6doc.com publ., ISBN 978-2-87587-090-2. Available from http://www.i6doc.com/en/.

the measured EEG [5], however most traditional ICA algorithms are only suitable for offline use [6]. Band-pass filtering has been used to extract the relevant MI-related frequencies in the so called the mu (μ) band (8-12Hz) signals. This frequency band is characterized for exhibiting a phenomenon called event-related desynchronization (ERD), attenuation of the power, in the contralateral motor cortex during the imagination of upper limb movement [7].

Multiple studies have reported the use of Common Spatial Patterns (CSP) method for feature extraction [8, 9]. This method applies a spatial filter to transform the original signal into two components which are optimal in the least squares sense for discriminating two classes [10]. After CSP feature extraction, classifiers like Linear Discriminant Analysis (LDA), Support Vector Machines and Random Forest are very common choices [11].

The majority of the BCIs are based only on sensor space analysis [11]. At the sensor level, the EEG is characterized by a low spatial resolution due to the volume conduction problem [12]. This results in spatial mixing in the measured EEG signal. EEG Source Imaging (ESI) methods can be used to estimate the potentials generated on the brain cortex and provide an unmixed localization and time-courses of the underlying sources. The integration of ESI methods into MI-based BCIs has been scarcely reported, though some studies [9, 13, 14] that have reported that source space analysis leads to an improvement of the classification of MI.

In this study, we have evaluated traditional and novel pipelines in both sensor and source spaces for classifying upper limb MI. Notably, we introduce the use of average power over regions-of-interest (ROI) as key feature in the source space, demonstrating a distinctive approach with ESI that surpasses conventional analysis done only in sensor space.

2 Materials and Methods

2.1 Motor Imagery EEG Dataset

A pool of 10 subjects of the MI dataset from GigaScience database [15] was used to evaluate the classification performance. The data was collected during performance of hand MI imagery tasks with a sampling frequency of 512 Hz, and using 64 Ag/AgCl active electrodes distributed over the scalp using the standard 10-10 montage. Each subject performed 100 or 120 trials of motor imagery from each class; right and left MI. Each trial lasts 7s: 2s corresponds to a fixation cross, 3s of MI task after a cue of right or left is presented, and 2s of blank screen. The data was handled using MNE-python [16], and it was divided into epochs of equal length between -2s and 5s around the MI cue.

2.2 Evaluation Pipelines

A total of 4 pipelines were evaluated in this study, 2 using only sensor space analysis and 2 including source space analysis. The pipelines consist of 5 steps after data collection: artifact removal using ICA; mu-band frequency filtering using band-pass filter; analysis space definition, either using ESI or left as-is in

ESANN 2024 proceedings, European Symposium on Artificial Neural Networks, Computational Intelligence and Machine Learning. Bruges (Belgium) and online event, 9-11 October 2024, i6doc.com publ., ISBN 978-2-87587-090-2. Available from http://www.i6doc.com/en/.

the sensor space; feature extraction, either using CSP or average channel/source power; and classification using LDA. The pipelines are illustrated in Fig. 1.

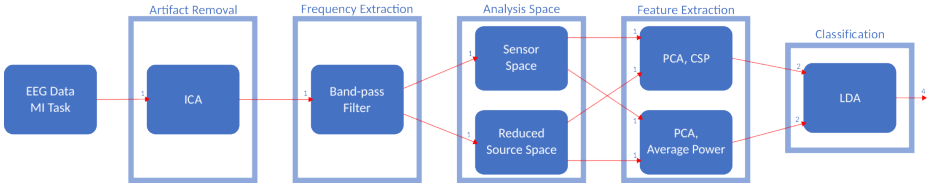

Fig. 1: Analysis Pipelines from Raw EEG Data of the MI task to classification. Numbers indicate the number of different combinations of methods result after each step.

Artifact removal - ICA was performed individually on each subject, using MNE-Python's ICA tool with the Picard method [17]. Prior to ICA, all epochs were high-pass filtered at 0.5Hz to remove baseline drift. Epochs marked as "bad" in the dataset were removed, along with epochs with a peak-to-peak value higher than 200μV. The transformed data was inspected visually to find any independent components which contained common ocular artifacts. Lateral eye movement and blinks were identified and excluded from the data.

Filtering - A zero-phase bandpass filter with cutoff frequencies 8-12Hz was applied to the epochs in each pipeline to extract the information of the mu band.

Analysis space definition -The analysis space refers that the features were extracted directly from the EEG channels (sensor space) or from the ESI estimation (source space). For the sensor space analysis, the complete set 64 EEG channels were used. For the source space, the source activity was estimated using the Dynamic Statistical Parametric Mapping (dSPM) [18] method using a head model of 8196 sources, the epochs, and an ad-hoc diagonal covariance matrix. The head model was computed using the boundary element model over the so-called fsaverage subject's magnetic resonance imaging (MRI) data, available in MNE-python. A smaller subset of sources located in and around the motor cortex was defined using Destrieux atlas [19] for automatic parcellation. This subset is here referred to as the reduced source space and it contains sources from the following ROIs: the paracentral lobule and sulcus, the subcentral gyrus, the long insular gyrus, the post- and precentral gyrus, the central and postcentral sulcus and the inferior and superior part of the precentral sulcus. The names and locations of the selected ROIs are represented by the colored regions color in Fig. 2. After selection the sources within the ROIs, the set of sources was reduced to 1251.

Feature extraction - CSP was applied in the reduced source space and the sensor space, in the interval $t \in [0.5, 3]s$. For each vertex or channel j, the average power p^j was calculated using $p^j = \frac{1}{N}\sum_{i=1}^{N}\left|x_i^j\right|^2$, where x_i^j is the i-th sample in the interval $t \in [0.5, 3]s$ and was used as the feature vector for classification. Principal component analysis (PCA) was used in conjunction with both feature extraction methods to reduce computational load, reduce the

ESANN 2024 proceedings, European Symposium on Artificial Neural Networks, Computational Intelligence and Machine Learning. Bruges (Belgium) and online event, 9-11 October 2024, i6doc.com publ., ISBN 978-2-87587-090-2. Available from http://www.i6doc.com/en/.

curse of dimensionality.

Classification - This step was performed using LDA classifier. 20% of the epochs from each subject were kept aside as a test set. The remaining epochs were used for 5-fold stratified cross-validation with a 80-20% training-validation split, which was used for finding the optimal number of principal components.

Statistical analysis - The classification means were bootstrapped and compared using a pairwise Dunn's test [20].

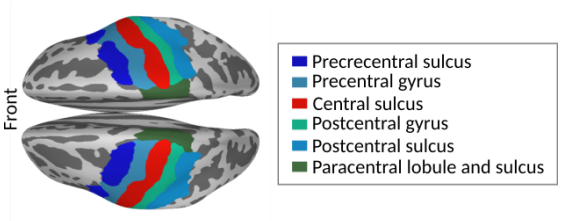

Fig. 2: Top view of the selected ROIs (colored regions) around the motor and sensory cortex.

3 Results and Discussion

The classification accuracy from the pipelines is summarized in Fig. 3, which illustrates the individual and mean test accuracy for each classification pipeline. Overall the best average classification accuracy is 80.1%, which was achieved using average power in the source space as features, followed by CSP in source and sensor space both with 70.3%, and average power in sensor space with 70.0%. Interestingly, the average accuracy significantly increases by approximately 10% when going from the average power in the sensor space to the source space, similarly when comparing against CSP in sensor and source spaces. When inspecting subject by subject, it is noticeable that for most of the subjects the best accuracy obtained was when using ESI in the pipeline.

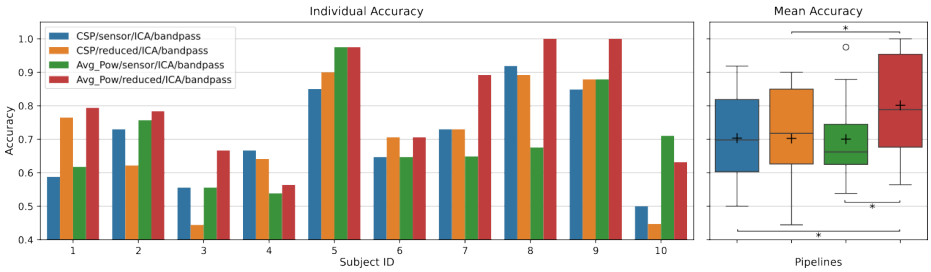

Fig. 3: Test set classification accuracy of each pipeline. Left: Individual accuracy. Right: Group accuracy per pipeline. + represents the mean accuracy and $*$ represents statistical significance $p < 0.05$ (Bootstrapping and Dunn's test).

The results indicate that higher classification can be achieved when involving ESI and applying feature extraction over the source space, where using the reduced source space gave significantly higher classification accuracy than the sensor space when using average power as feature. The results are in line with the

ESANN 2024 proceedings, European Symposium on Artificial Neural Networks, Computational Intelligence and Machine Learning. Bruges (Belgium) and online event, 9-11 October 2024, i6doc.com publ., ISBN 978-2-87587-090-2. Available from http://www.i6doc.com/en/.

findings in [9], where similar pipelines ICA, Band-pass, CSP, and sensor space or source space based on identified activation regions. In that study ESI was computed with weighted minimum norm estimation (wMNE), and the evaluation was performed over a pool of 10 subjects of the same dataset used here. The study presented an average classification accuracy for MI of 74.0% and 79.2% for sensor and source spaces, respectively. Here, using an ROIs approach instead of activation regions and ESI with dSPM, the best accuracy considering the closest pipelines were 70.3% with both sensor and reduced source space. However, when varying the pipeline including average power on the source space, the accuracy increased up to 80.3%.

In this work we introduce the average power as feature for MI classification. The use of the average power as feature has improved significantly the classification accuracy in the source space when comparing with CSP. While not tested in this study, other algorithms could have been used for ESI, as algorithms differ in assumptions and approaches when estimating the source activity [21, 22], it is therefore interesting to investigate ESI algorithms' influence in future research. Here the ROIs were defined a priori for source space and the complete set of electrodes was used in the sensor space, optimization [23, 24] of sensor and source space should be explored in future studies to determine the most influential ROIs and sensors in combination with the average power.

4 Conclusion

In conclusion, the results presented in this work suggest that the source space can provide suitable information that allows to achieve higher classification accuracy on MI classification when compared to the sensor space. We have introduced the feature of average power on source space using ESI, being a key element for the accuracy increase. To the best of our knowledge this has not been used as a feature when combined with ESI.

References

[1] J. J. Vidal, "Toward direct brain-computer communication," *Annual Review of Biophysics and Bioengineering*, vol. 2, no. 1, pp. 157–180, 1973, pMID: 4583653.

[2] T. Yanagisawa, R. Fukuma, B. Seymour, M. Tanaka, K. Hosomi, O. Yamashita, H. Kishima, Y. Kamitani, and Y. Saitoh, "BCI training to move a virtual hand reduces phantom limb pain: A randomized crossover trial," *Neurology*, vol. 95, no. 4, pp. e417–e426, 07 2020.

[3] W. Liao, J. Li, X. Zhang, and C. Li, "Motor imagery brain-computer interface rehabilitation system enhances upper limb performance and improves brain activity in stroke patients: A clinical study," *Frontiers in Human Neuroscience*, vol. 17, 2023.

[4] F. Campos Viola, J. Thorne, B. Edmonds, T. Schneider, T. Eichele, and S. Debener, "Semi-automatic identification of independent components representing eeg artifact," *Clinical Neurophysiology*, vol. 120, no. 5, pp. 868–877, 2009.

[5] J. Uriguen and B. Garcia-Zapirain, "Eeg artifact removal state-of-the-art and guidelines," *Journal of Neural Engineering*, vol. 12, no. 3, p. 031001, 04 2015.

[6] X. Lin, L. Wang, and T. Ohtsuki, "Online recursive ica algorithm used for motor imagery eeg signal," in *2020 42nd Annual International Conference of the IEEE Engineering in Medicine & Biology Society (EMBC)*, 2020, pp. 502–505.

ESANN 2024 proceedings, European Symposium on Artificial Neural Networks, Computational Intelligence and Machine Learning. Bruges (Belgium) and online event, 9-11 October 2024, i6doc.com publ., ISBN 978-2-87587-090-2. Available from http://www.i6doc.com/en/.

[7] G. Pfurtscheller, C. Brunner, A. Schlogl, and F. Lopes da Silva, "Mu rhythm (de)synchronization and eeg single-trial classification of different motor imagery tasks," *NeuroImage*, vol. 31, no. 1, pp. 153–159, 2006.

[8] J. Pereira, P. Ofner, A. Schwarz, A. I. Sburlea, and G. R. Müller-Putz, "Eeg neural correlates of goal-directed movement intention," *NeuroImage*, vol. 149, pp. 129–140, 4 2017.

[9] A. Giri, L. Kumar, and T. K. Gandhi, "Cortical source domain based motor imagery and motor execution framework for enhanced brain computer interface applications," *IEEE Sensors Letters*, vol. 5, no. 12, pp. 1–4, 2021.

[10] H. Ramoser, J. Müller-Gerking, and G. Pfurtscheller, "Optimal spatial filtering of single trial eeg during imagined hand movement," *IEEE Transactions on Rehabilitation Engineering*, vol. 8, no. 4, pp. 441–446, 2000.

[11] F. Lotte, L. Bougrain, A. Cichocki, M. Clerc, M. Congedo, A. Rakotomamonjy, and F. Yger, "A review of classification algorithms for eeg-based brain–computer interfaces: a 10 year update," *Journal of Neural Engineering*, vol. 15, p. 031005, 4 2018.

[12] R. Portillo-Lara, B. Tahirbegi, C. Chapman, J. Goding, and R. Green, "Mind the gap: State-of-the-art technologies and applications for eeg-based brain–computer interfaces," *APL Bioengineering*, vol. 5, p. 031507, 09 2021.

[13] N. Srisrisawang and G. R. Müller-Putz, "Applying dimensionality reduction techniques in source-space electroencephalography via template and magnetic resonance imaging-derived head models to continuously decode hand trajectories," *Frontiers in Human Neuroscience*, vol. 16, p. 137, 3 2022.

[14] B. J. Edelman, B. Baxter, and B. He, "Eeg source imaging enhances the decoding of complex right-hand motor imagery tasks," *IEEE Transactions on Biomedical Engineering*, vol. 63, pp. 4–14, 1 2016.

[15] H. Cho, M. Ahn, S. Ahn, M. Kwon, and S. C. Jun, "Eeg datasets for motor imagery brain–computer interface," *GigaScience*, vol. 6, no. 7, p. gix034, 05 2017.

[16] A. Gramfort, M. Luessi, E. Larson, D. A. Engemann, D. Strohmeier, C. Brodbeck, R. Goj, M. Jas, T. Brooks, L. Parkkonen, and M. S. Hämäläinen, "MEG and EEG data analysis with MNE-Python," *Frontiers in Neuroscience*, vol. 7, no. 267, pp. 1–13, 2013.

[17] P. Ablin, J. F. Cardoso, and A. Gramfort, "Faster independent component analysis by preconditioning with hessian approximations," *IEEE Transactions on Signal Processing*, vol. 66, pp. 4040–4049, 8 2018.

[18] A. M. Dale, A. K. Liu, B. R. Fischl, R. L. Buckner, J. W. Belliveau, J. D. Lewine, and E. Halgren, "Dynamic statistical parametric mapping: Combining fmri and meg for high-resolution imaging of cortical activity," *Neuron*, vol. 26, pp. 55–67, 4 2000.

[19] C. Destrieux, B. Fischl, A. Dale, and E. Halgren, "Automatic parcellation of human cortical gyri and sulci using standard anatomical nomenclature," *NeuroImage*, vol. 53, no. 1, pp. 1–15, 2010.

[20] O. J. Dunn, "Multiple comparisons using rank sums," *Technometrics*, vol. 6, no. 3, pp. 241–252, 1964.

[21] C. M. Michel and D. Brunet, "EEG source imaging: A practical review of the analysis steps," *Frontiers in Neurology*, vol. 10, no. APR, p. 325, apr 2019.

[22] A. Soler, P. A. Muñoz-Gutiérrez, M. Bueno-López, E. Giraldo, and M. Molinas, "Low-density eeg for neural activity reconstruction using multivariate empirical mode decomposition," *Frontiers in Neuroscience*, vol. 14, 2020.

[23] A. Soler, L. A. Moctezuma, E. Giraldo, and M. Molinas, "Automated methodology for optimal selection of minimum electrode subsets for accurate EEG source estimation based on Genetic Algorithm optimization," *Scientific Reports 2022 12:1*, vol. 12, no. 1, pp. 1–18, jul 2022.

[24] A. Soler, E. Giraldo, and M. Molinas, "Eeg source imaging of hand movement-related areas: an evaluation of the reconstruction and classification accuracy with optimized channels," *Brain Informatics 2024 11:1*, vol. 11, pp. 1–12, 5 2024.